Self-Assembly in Helical Columnar Mesophases and Luminescence of Chiral 1H-Pyrazoles

ARTICLE *in* CHEMISTRY - A EUROPEAN JOURNAL · AUGUST 2009

Impact Factor: 5.73 · DOI: 10.1002/chem.200901154 · Source: PubMed

6 AUTHORS, INCLUDING:

Emma Cavero
Industrias Químicas del Ebro
19 PUBLICATIONS **303** CITATIONS
SEE PROFILE

Jose Luis Serrano
University of Zaragoza
369 PUBLICATIONS **7,534** CITATIONS
SEE PROFILE

DOI: 10.1002/chem.200901154

Self-Assembly in Helical Columnar Mesophases and Luminescence of Chiral 1*H*-Pyrazoles

Eduardo Beltrán,[a] Emma Cavero,[a] Joaquín Barberá,[a] José Luis Serrano,[a] Anabel Elduque,*[b] and Raquel Giménez*[a]

Abstract: Chiral polycatenar 1*H*-pyrazoles self-assemble to form columnar mesophases that are stable at room temperature. X-ray diffraction and CD studies in the mesophase indicate a supramolecular helical organization consisting of stacked H-bonded dimers. The liquid-crystalline compounds reported are 3,5-bis(dialkoxyphenyl)-1*H*-pyrazoles that incorporate two or four dihydrocitronellyl chiral tails. It can be observed that the grafting of these branched chiral substituents onto the 3,5-diphenyl-1*H*-pyrazole core has a beneficial role in inducing mesomorphism, because isomeric linear-chain compounds are not liquid crystalline; this is not the usual scheme of behavior. Furthermore, the molecular chirality is transferred to the columnar mesophase, because preferential helical arrangements are observed. Films of the compounds are luminescent at room temperature and constitute an example of the self-organization of nondiscoid units into columnar liquid-crystalline assemblies in which the functional molecular unit transfers its properties to a hierarchically built superstructure.

Keywords: chirality · liquid crystals · luminescence · nanostructures · self-assembly · supramolecular chemistry

Introduction

The self-assembly of molecular building blocks into complex ordered systems is a subject of increasing research interest and underpins the development of bottom-up approaches to functional nanostructures.[1–4] The information encoded in the molecular components is fundamental in yielding structures through supramolecular interactions, with exquisite control of shape and function.

Complex supramolecular arrangements can be obtained from simple molecules by means of noncovalent interactions, which encompass H-bonding, dipolar forces, Coulombic interactions, π–π stacking, metal complexation, or a combination of these. Chirality is another powerful element to yield extended hierarchical organizations and functions.[5] All of these characteristics are put into play in columnar liquid crystals, in which molecular or supramolecular entities are stacked and the molecular chirality can be transferred and amplified through the formation of helical superstructures.[6] Moreover, desirable optical and electronic properties can be attained with columnar organizations consisting of functional molecular entities.[7–12]

1*H*-Pyrazoles are structural building blocks that have the potential to self-organize into a rich variety of superstructures through hydrogen bonding.[13] As part of our research program, we have studied polycatenar 3,5-diaryl-1*H*-pyrazoles as promesogenic ligands in coordination compounds with boron,[14,15] gold,[16,17] zinc,[18] and rhodium[19] in order to obtain columnar mesophases. All of the complexes reported were liquid crystalline, despite the variety of shapes and geometries, with the mesophases obtained at room temperature in most cases. However, the 1*H*-pyrazoles themselves were not liquid crystalline, despite their elongated rigid shape and the possibility of generating stackable dimeric or trimeric structures by H-bonding. We therefore concluded that H-bonding, although present in the condensed phases of the 1*H*-pyrazoles, was not sufficient to induce and stabilize the columnar stacking of molecules with such low aspect ratios.

In the work described here, we successfully attempted to induce columnar mesophases in purely organic 3,5-diaryl-

[a] E. Beltrán, Dr. E. Cavero, Dr. J. Barberá, Prof. J. L. Serrano, Dr. R. Giménez
Department of Organic Chemistry
Facultad de Ciencias—Instituto de Ciencia de Materiales de Aragón
Universidad de Zaragoza—CSIC, Pedro Cerbuna 12, 50009 (Spain)
Fax: (+34) 976-762686
E-mail: rgimenez@unizar.es

[b] Dr. A. Elduque
Department of Inorganic Chemistry
Facultad de Ciencias—Instituto de Ciencia de Materiales de Aragón
Universidad de Zaragoza—CSIC, Pedro Cerbuna 12, 50009 (Spain)

1*H*-pyrazoles through the introduction of branched chiral chains. In particular, the structures studied consist of 3,5-bis-(alkoxyphenyl)-1*H*-pyrazoles that incorporate several chiral (3,7-dimethyloctyl, also named dihydrocitronellyl) and/or achiral (*n*-decyloxyl) aliphatic side chains, with the total number ranging from four to six (Scheme 1). From the

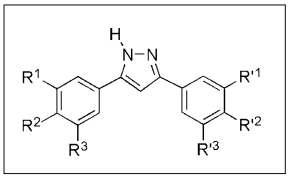

4(*S*): $R^1 = R'^1 = R^2 = R'^2 =$ 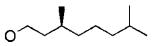 $R^3 = R'^3 = H$

4(*R*): $R^1 = R'^1 = R^2 = R'^2 =$ 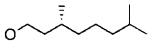 $R^3 = R'^3 = H$

5(*S*): $R^1 = R'^1 = R^2 = R'^2 = R^3 =$ 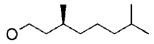 $R'^3 = H$

6(*S*): $R^1 = R'^1 = R^2 = R'^2 = R^3 = R'^3 =$ 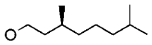

2(*S*)2C10: $R^1 = R^2 =$ 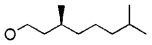 $R'^1 = R'^2 = n$-decyloxyl $R^3 = R'^3 = H$

2(*R*)2C10: $R^1 = R^2 =$ 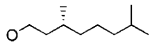 $R'^1 = R'^2 = n$-decyloxyl $R^3 = R'^3 = H$

2(*S*)3C10: $R^1 = R^2 =$ 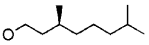 $R'^1 = R'^2 = R'^3 = n$-decyloxyl $R^3 = H$

3(*S*)2C10: $R^1 = R^2 = R^3 =$ 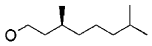 $R'^1 = R'^2 = n$-decyloxyl $R'^3 = H$

3(*S*)3C10: $R^1 = R^2 = R^3 =$ 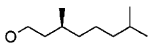 $R'^1 = R'^2 = R'^3 = n$-decyloxyl

Scheme 1. Molecular structures of the chiral 1*H*-pyrazoles.

structural characterization, we propose that H-bonded dimeric species are present as the secondary structure of the compounds and that these species, in turn, self-assemble at room temperature to give thermodynamically stable columnar liquid-crystalline assemblies with helical organization. We also show that films of these compounds exhibit luminescence in the mesophase, and this constitutes an example in which the functional molecular unit (3,5-diphenylpyrazole) transfers its properties to a hierarchically built superstructure.

Results and Discussion

Synthesis: The synthesis of polycatenar 1*H*-pyrazoles is accomplished by the reaction of 1,3-diketones with hydrazine hydrate. The precursor 1,3-diaryl-1,3-diketones have traditionally been obtained by Claisen condensation of an acetophenone and a benzoate ester with NaH in 1,2-dimethoxyethane heated to reflux. However, this reaction often gives low yields and extensive hydrolysis of the benzoate ester, and it is very sensitive to the storage conditions of NaH. For this reason, we prepared the pyrazoles described in this work by adapting a recently described one-pot procedure[20] to our polyalkoxy starting materials. The method uses a weaker base (lithium 1,1,1,3,3,3-hexamethyldisilazane or LiHMDS) to generate the enolate of the acetophenone, low temperatures, and acid chlorides, which are better electrophiles than esters. The diketone was not isolated but was treated directly with hydrazine hydrate to give the final 1*H*-pyrazole (Scheme 2).

Self-assembly and structural characterization: Compounds **2(*S*)2C10** and **2(*R*)2C10**, with two *n*-decyloxyl tails and two dihydrocitronellyl tails, were isolated as liquid-crystalline materials that crystallized after several weeks. Polarizing optical microscopy and differential scanning calorimetry (DSC) studies revealed that both enantiomers display a columnar mesophase with pseudo-focal-conic textures on cooling from the isotropic liquid (Figure 1). Isomeric compounds **4(*S*)** and **4(*R*)**, with four dihydrocitronellyl tails, are thermodynamically stable columnar liquid crystals at room temperature (Table 1). The terminal chain structure is fundamental in inducing mesomorphism, because the isomeric linear-chain pyrazole (with four *n*-decyloxyl tails) is solid at room temperature and melts to an isotropic liquid at 95 °C with a high enthalpy.[21] The pyrazoles with five chains (**2(*S*)3C10**, **3(*S*)2C10**, and **5(*S*)**) are all isotropic liquids at room temperature and glassify with no signs of crystallization or meso-

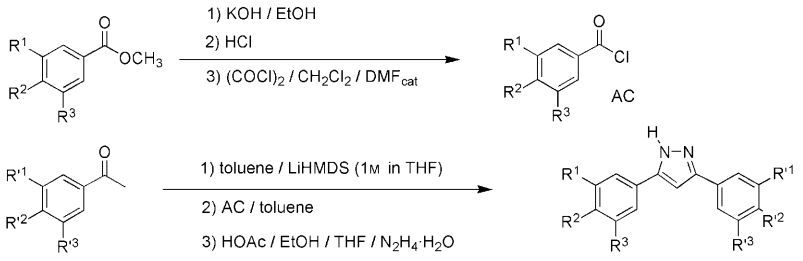

Scheme 2. Synthetic pathway for the polycatenar 1*H*-pyrazoles. DMF: *N*,*N*-dimethylformamide; THF: tetrahydrofuran.

phase induction below room temperature. This is in sharp contrast with the isomeric compound bearing five *n*-decyloxyl tails, which is a solid and melts to an isotropic liquid at 57 °C.[15] Pyrazoles with six alkoxy tails (**3(*S*)3C10** and **6(*S*)**) are isotropic liquids at room temperature, as is the isomeric pyrazole with six *n*-decyloxyl tails.[15]

Therefore, only the introduction of dihydrocitronellyl chains in the compounds with four chains gives rise to a decrease in the melting point and the induction of mesomorphism, which provides evidence that the columnar organizations found with these molecules result from a delicate bal-

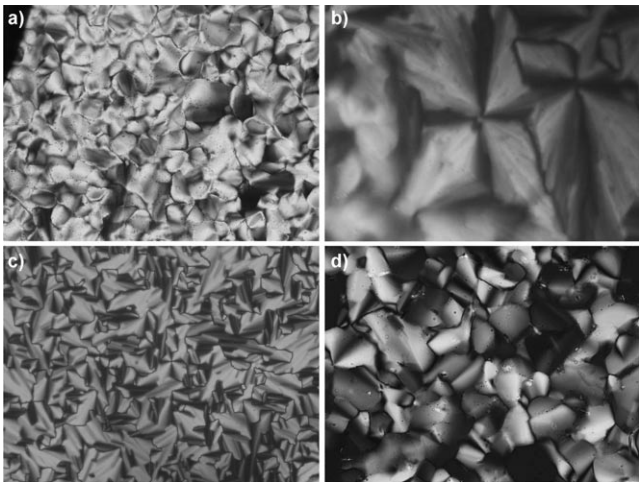

Figure 1. Microphotographs of the mesophases observed at room temperature for a) **2(*S*)2C10**, b) **2(*R*)2C10**, c) **4(*S*)**, and d) **4(*R*)**.

Table 1. DSC data for the mesomorphic 1*H*-pyrazoles.[a]

Compound	Thermal cycle	Peak phase-transition temperatures [°C] (transition enthalpies [kJ mol^{-1}])
2(*S*)2C10	1st heating	Cr[b] 58 (54.9) I
	1st cooling	I 38 (1.2) Colh
	2nd heating	Colh 47 (1.3) I
2(*R*)2C10	1st heating	Cr[b] 58 (45.3) I
	1st cooling	I 39 (1.9) Colh
	2nd heating	Colh 47 (1.8) I
4(*S*)	1st heating	Colh 57 (2.6) I
4(*R*)	1st heating	Colh 56 (2.3) I
2(*S*)3C10	1st heating	I[c]
3(*S*)2C10	1st heating	I[c]
5(*S*)	1st heating	I[c]
3(*S*)3C10	1st heating	I[c]
6(*S*)	1st heating	I[c]

[a] Cr: crystalline phase; Colh: columnar hexagonal mesophase; I: isotropic liquid. [b] Transition only observed after the crystalline phase had been left for several weeks at room temperature. [c] Isotropic liquid at room temperature. No DSC peaks were detected below room temperature.

ance of weak supramolecular van der Waals side-chain interactions, space filling, and H-bonding. This is contrary to the usual scheme of behavior, in that a decrease of the transition temperatures caused by dihydrocitronellyl groups usually reduces the mesophase interval relative to that of the analogous linear-chained columnar liquid crystals, due to the existence of an increased degree of side-chain disorder.[22] However, it is worth mentioning that for some well-established discotic liquid crystals, like triphenylenes[23] or coronenes,[24] stabilization of the columnar mesophase and increased order has been observed upon the introduction of branched lateral chains; this was attributed to an improvement in the peripheral space filling around the aromatic cores.

Powder X-ray diffraction (XRD) studies in the mesophase were performed at room temperature on all compounds that have a stable mesophase at that temperature, including **2(*S*)2C10** and **2(*R*)2C10**, for which no signs of crystallization were observed during the experiments. The experiments confirmed that the mesophase of the pyrazoles with four chains is hexagonal columnar (Table 2). The hexagonal cell

Table 2. Powder X-ray diffraction data (*d*) for the mesophase at room temperature.

Compound	$d_{measured}$ [Å]	d_{calcd} [Å]	*hk*	Mesophase parameters
2(*S*)2C10 and **2(*R*)2C10**	22.8	22.9	10	Colh, $a=26.4$ Å
	13.3	13.2	11	
	11.5	11.5	20	
	4.6			
4(*S*) and **4(*R*)**	21.5	21.3	10	Colh, $a=24.6$ Å
	12.4	12.3	11	
	10.5	10.6	20	
	4.6			

parameter is slightly smaller for the all-dihydrocitronellyl-substituted compounds **4(*S*)** and **4(*R*)**, due to the shorter length of the aliphatic tails in comparison with that of the *n*-decyloxyl tails.

A study on a partially aligned sample of compound **2(*S*)2C10** revealed that the columns were oriented parallel to the capillary axis and, hence, perpendicular to the X-ray beam. In the oriented pattern (Figure 2a), a sharp maximum

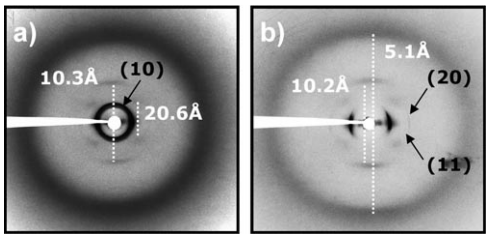

Figure 2. XRD patterns for the mesophase of a) **2(*S*)2C10** and b) **4(*S*)**.

appeared in the low-angle region; this can be assigned to the (10) reflection from the two-dimensional hexagonal lattice. A diffuse halo, which is characteristic of the liquid-like order of the aliphatic chains, was also observed at wide angles (4.6 Å). The low-angle maximum is reinforced in the equatorial region (plane perpendicular to the capillary axis).

In addition, a set of spots at middle angles was also observed. These appeared in the meridional region (parallel direction to the column axes), and they are related to the periodic distances or local order within the column. The pair of diffuse spots that appear at both sides of the meridian at middle angles are indicative of a modulation of the electronic density along the stacking direction. We attribute the modulation to a helical stacking of the molecules in the column.[25–31] The periodicity of the modulation is 20.6 Å and corresponds to the periodicity of the helix.

The supramolecular organization in the columnar mesophase can be envisaged by estimating the number of molecules related to the periodicity of 20.6 Å in a hexagonal cell

with $a = 26.4$ Å, which amounts to 8 for a density of about 1 g cm^{-3}. This finding allowed us to propose a model with 2 pyrazoles per column stratum and a mean stacking distance of 5.2 Å. The two pyrazoles could interact through a double intermolecular H-bond, which would give rise to a discotic dimer. The size of the discotic dimer agrees well with the measured hexagonal parameter for this mesophase (see Table 2) and is fully consistent with the cell parameters previously measured in hexagonal columnar mesophases of similar derivatives, for example, the covalently bound pyrazole dimers derived from bis(pyrazolyl)methane ($a = 28.2$ Å)[18] or the mononuclear rhodium–pyrazole complex with an antiparallel arrangement of molecules along the column ($a =$ 27.0 Å).[19]

This situation is further supported by the fact that the NH-stretching peak in the IR spectrum appears in the H-bonded region (below 3200 cm^{-1}). If the 1*H*-pyrazoles interact by H-bonding in their solid state, this could give rise to different structures depending on the steric and polarizability effects of their substituents.[13,32] In particular, 3,5-diarylpyrazoles have been found to interact in dimers by double intermolecular H-bonds[33–35] or in tetramers by four intermolecular H-bonds.[19,35,36] The dimeric species are planar, but the tetrameric systems are globular and are therefore less suitable for stacking in columns.

The data are consistent with a columnar structure in which the stacked dimers are mutually rotated around the normal to their mean planes by an angle of 45° (Figure 3). If their two-fold symmetry is taken into account, 4 dimers make half a turn and, thus, the actual helical pitch is 41.2 Å. The additional sharp and intense maximum appearing at 10.3 Å at the meridian is consistent with a certain local order along the column, and this corresponds to twice the stacking distance (5.2 Å × 2). This could be due to a modulation of the electronic density along the column arising from an interaction between the aromatic rings of one pyrazole and its second nearest neighbor, which is rotated by 90° (Figure 3). Indeed, due to the X-like shape of the dimers, the benzene rings of every two stacked molecules are located on top of each other. The same orientation pattern was observed for compound **2(*R*)2C10**, which afforded a similar superstructure.

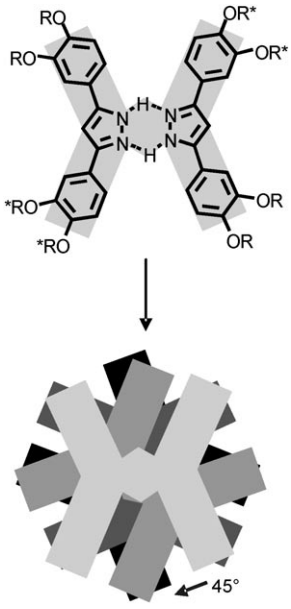

Figure 3. Schematic representation of the dimeric association and proposed molecular model for the columnar packing.

In the case of the all-chiral compounds, we were able to obtain a well-oriented pattern for **4*S***, and this confirmed that a helical organization also exists in the columnar mesophase. In this case (Figure 2b), we could observe up to the third order of a hexagonal symmetry along the equator; a split scattering maximum assigned to the helical structure at 20.0 Å; and meridional reflections at 10.2 and 5.1 Å assigned to additional electronic modulation along the stacking direction. These observations are consistent with the model proposed in Figure 3, in which dimers are stacked regularly at 5.1 Å and arranged in a helical fashion with a pitch of 40 Å.

Optical properties: Absorption spectra were measured on films of the 1*H*-pyrazoles at room temperature. The data are collected in Table 3. In all cases, 2 main broad bands were observed, the first centered at around 220 nm and the second at 270 nm. The latter band has a shoulder at 300 nm in the compounds with 5 or 6 aliphatic chains (samples that are in the isotropic liquid state), but it is much broader, with a second shoulder at 310 nm, for the compounds with 4 chains (which are measured in the columnar mesophase) as a consequence of the supramolecular aggregation.

Table 3. Absorption (λ_{abs}) and emission data (λ_{em}) for film samples at room temperature.

Compound	λ_{abs}[a] [nm]	λ_{em} [nm]
2(*S*)2C10	218, 267, 293^{sh}, 310^{sh}	350
2(*R*)2C10	218, 267, 293^{sh}, 310^{sh}	350
4(*S*)	219, 270, 301^{sh}, 314^{sh}	347
4(*R*)	219, 268, 301^{sh}, 314^{sh}	347
2(*S*)3C10	225, 260, 298^{sh}	344
3(*S*)2C10	223, 263, 299	344
5(*S*)	214, 272, 300	342
3(*S*)3C10	221, 274, 300	351
6(*S*)	219, 302	353

[a] sh: shoulder band.

The compounds exhibit a broad luminescence band in the near-UV blue region when excited at either their absorption maxima or at longer wavelengths (Figure 4). All of the compounds display similar behavior, independently of their physical state, and the spectra are related to the molecular emission bands, which indicates little effect of the condensed phase on the emission wavelength.

Circular dichroism (CD) and UV/Vis spectra of thin films were measured in the hexagonal columnar phase in an effort to prove further the existence of chiral supramolecular structures. The samples were prepared on a quartz

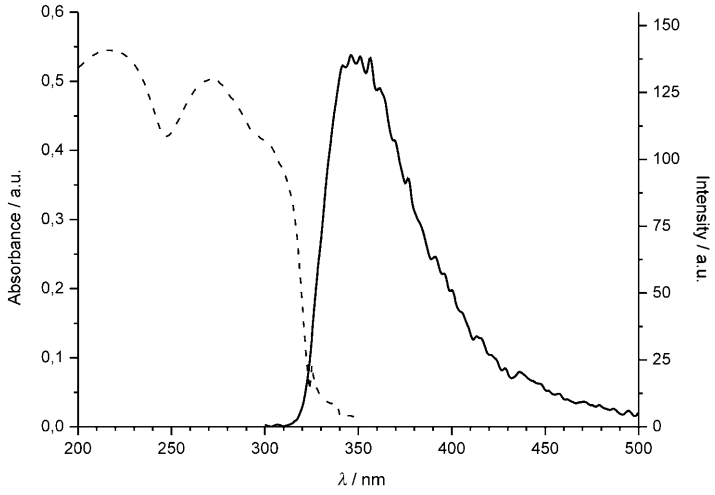

Figure 4. Absorption (dashed line) and emission (solid line) spectra of the mesophase of **2(*S*)2C10** at room temperature.

plate, heated to form the isotropic liquid, and cooled to room temperature. The averaged CD spectra of compounds **4(*S*)** and **4(*R*)** show bands in the region of the absorption of the compound (Figure 5). These bands are not present in

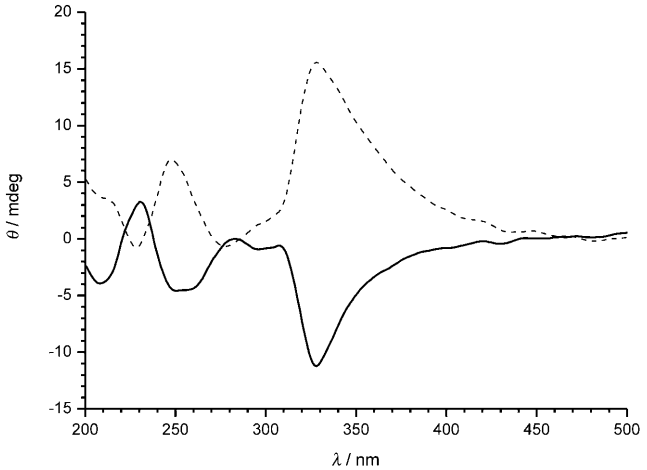

Figure 5. CD spectra of the mesophase of **4(*S*)** (dashed line) and **4(*R*)** (solid line) at room temperature.

the isotropic melt or in solution, and the main signals observed are related to wavelengths at which the UV/Vis spectra show aggregation bands. When the compound bears the enantiomeric chiral tail (**4(*S*)** versus **4(*R*)**), the CD spectrum obtained under the same conditions shows the opposite sign. Therefore, formal optical activity is observed, and this arises from a chiral superstructure in the mesophase that could indeed correspond to a helical arrangement within the column, as proposed from the oriented XRD pattern. Therefore, the molecular chirality is transferred to the columnar mesophase, because preferential helical arrangements of opposite handness, depending on the chirality sign of the dihydrocitronellyl side group, are observed.

For compounds **2(*S*)2C10** and **2(*R*)2C10**, although helical features were observed in the mesophase by XRD, the CD spectra measured under the same conditions as before do not show any signal. We attribute this behavior to the fact that the helical organization present is not biased towards any prevailing twist sense in these compounds.

Conclusions

We have shown that nondiscoid 3,5-diaryl-1*H*-pyrazoles bearing dihydrocitronellyl chiral tails display columnar mesophases at room temperature only if the compound contains two dihydrocitronellyl chains and two *n*-decyloxyl chains or, alternatively, four dihydrocitronellyl chains. Other combinations do not yield liquid-crystalline assemblies, which provides evidence that the columnar organizations found in these compounds result from a delicate balance of weak supramolecular van der Waals interactions and H-bonding.

The current observations point to a hierarchical self-assembly in which the 1*H*-pyrazoles self-assemble into disk-like dimers through double intermolecular hydrogen bonds. These dimers stack to form hexagonal columnar structures, which in turn have a helical structure. Films of these compounds exhibit luminescence in the mesophase. This constitutes an example of the self-organization of nondiscoid functional units into columnar liquid-crystalline assemblies.

Experimental Section

Methods: The XRD patterns were obtained with a pinhole camera (Anton–Paar) operating with a point-focused Ni-filtered Cu-Kα beam. The samples were held in Lindemann glass capillaries (0.9 mm diameter), and the patterns were collected on flat photographic film perpendicular to the X-ray beam. Spacings were obtained by using Bragg's law.

Materials: Acetophenones and benzoates were prepared according to methods previously reported for polyalkoxylated compounds.[15] Polyalkoxylated acid chlorides were prepared by hydrolysis of the benzoates to form the benzoic acids and reaction with oxalyl chloride. The chiral alkoxy chains required for alkylation reactions were prepared by catalytic hydrogenation of the commercially available (*R*)- or (*S*)-citronellyl bromide.[37]

General procedure for the preparation of 1*H*-pyrazoles: LiHMDS (1.05 mmol, 1.05 mL of a 1 M solution in THF) was added dropwise to a cooled (0 °C) solution of the polyalkoxylated acetophenone (1 mmol) in dry toluene (10 mL) under argon. The mixture was stirred at 0 °C for 5 min, and then a solution of the corresponding acid chloride (1 mmol) in dry toluene (10 mL) was added by cannula. The reaction mixture was stirred at room temperature until completion (1–5 h). Acetic acid (2 mL), ethanol (10 mL), THF (5 mL), and hydrazine hydrate (17.2 mmol, 0.8 mL) were added, and the mixture was stirred at 80 °C for 2 h. The mixture was cooled to room temperature, poured into 1 M NaOH (50 mL), extracted with ethyl acetate (2×20 mL), dried, and evaporated to dryness. The resulting residue was purified by flash chromatography with the eluent indicated in each particular case.

2(*S*)2C10 and 2(*R*)2C10: Eluent: CH_2Cl_2; yield: 40%; ^{1}H NMR (400 MHz, $CDCl_3$): δ = 0.85–0.89 (m, 18H), 0.95 (d, J = 6.3 Hz, 6H), 1.14–1.40 (m, 36H), 1.40–1.75 (m, 10H), 1.77–1.94 (m, 6H), 3.98–4.12 (m, 8H), 6.67 (s, 1H), 6.89–6.92 (m, 2H), 7.20–7.22 (m, 2H), 7.25 ppm (m, 2H); ^{13}C NMR (100 MHz, $CDCl_3$): δ = 14.1, 14.2, 19.6, 19.7, 22.6, 22.6, 22.7, 24.7, 26.0, 26.0, 27.9, 29.2, 29.3, 29.4, 29.6, 29.7, 29.8, 29.9, 31.9, 36.2,

37.3, 39.2, 67.3, 67.5, 69.1, 69.2, 98.8, 110.8 (br), 113.5, 113.7, 118.1, 124.3 (br), 149.0, 149.1, 149.3 ppm; IR (neat, NaCl): $\tilde{\nu}$ = 3152 (br, N–H), 1614, 1593, 1511, 1486, (C=N, Ar C–C), 1256 cm^{-1} (C–O); MS (MALDI): *m/z*: 845.8 [M^+]; elemental analysis calcd for $C_{55}H_{92}N_2O_4$: C 78.15, H 10.97, N 3.31; found for **2(*S*)2C10**: C 78.09, H 10.86, N 3.23; found for **2(*R*)2C10**: C 78.27, H 10.95, N 3.26.

4(*S*) and 4(*R*): Eluent: hexane/ethyl acetate (8:1.7); yield: 60%; ^{1}H NMR (400 MHz, $CDCl_3$): δ = 0.87 (d, *J* = 6.5 Hz, 24H), 0.95 (d, *J* = 6.5 Hz, 12H), 1.08–1.38 (m, 24H), 1.42–1.72 (m, 12H), 1.57–1.69 (m, 4H), 4.00–4.14 (m, 8H), 6.68 (s, 1H), 6.92 (d, 2H, *J* = 8.3 Hz, 2H), 7.22 (dd, *J* = 8.3, 1.7 Hz, 2H), 7.25 ppm (d, *J* = 1.7 Hz, 2H); ^{13}C NMR (100 MHz, $CDCl_3$): δ = 19.7, 22.6, 22.7, 24.7, 28.0, 29.9, 36.2, 36.3, 37.4, 39.3, 67.6, 67.7, 99.3, 111.2, 113.7, 118.3, 124.3, 149.4, 149.4 ppm; IR (neat, NaCl): $\tilde{\nu}$ = 3162 (br, N–H), 1609, 1590, 1511 (C=N, Ar C–C), 1262 cm^{-1} (C–O); MS (MALDI): *m/z*: 845.9 [M^+]; elemental analysis calcd for $C_{55}H_{92}N_2O_4$: C 78.15, H 10.97, N 3.31; found for **4(*S*)**: C 78.01, H 10.95, N 3.29; found for **4(*R*)**: C 77.95, H 10.85, N 3.24.

2(*S*)3C10: Eluent: CH_2Cl_2/ethyl acetate (20:1); yield: 56%; ^{1}H NMR (400 MHz, $CDCl_3$): δ = 0.85–0.87 (m, 21H), 0.96 (d, *J* = 6.5 Hz, 6H), 1.10–1.18 (m, 6H), 1.20–1.37 (m, 48H), 1.42–1.61 (m, 8H), 1.61–1.93 (m, 12H), 3.97–4.11 (m, 10H), 6.68 (s, 1H), 6.90–6.92 (m, 3H), 7.20 (dd, *J* = 8.4, 1.7 Hz, 1H), 7.24 ppm (d, *J* = 2.0 Hz, 1H); ^{13}C NMR (100 MHz, $CDCl_3$): δ = 14.1, 19.7, 22.6, 22.7, 22.7, 24.7, 26.1, 26.1, 28.0, 29.4, 29.4, 29.4, 29.6, 29.6, 29.7, 29.7, 29.7, 29.9, 30.3, 31.9, 31.9, 36.2, 36.3, 37.3, 39.3, 67.6, 67.7, 69.3, 73.5, 100.0, 104.5, 111.3, 113.7, 118.4, 149.2, 153.5 ppm; IR (neat, NaCl): $\tilde{\nu}$ = 3133, 3108 (br, N–H), 1589, 1507 (C=N, Ar C–C), 1258 cm^{-1} (C–O); MS (MALDI): *m/z*: 1001.9 [M^+]; elemental analysis calcd for $C_{65}H_{112}N_2O_5$: C 77.95, H 11.27, N 2.80; found: C 77.72, H 10.99, N 2.86.

3(*S*)2C10: Eluent: CH_2Cl_2/ethyl acetate (100:1); yield: 20%; ^{1}H NMR (400 MHz, $CDCl_3$): δ = 0.86–0.88 (m, 24H), 0.93 (d, *J* = 6.5 Hz, 9H), 1.12–1.40 (m, 42H), 1.42–1.65 (m, 10H), 1.65–1.79 (m, 4H), 1.80–1.91 (m, 6H), 3.98–4.08 (m, 10H), 6.66 (s, 1H), 6.85–6.92 (m, 3H), 7.19 (d, *J* = 8.3 Hz, 1H), 7.23 ppm (brs, 1H); ^{13}C NMR (100 MHz, $CDCl_3$): δ = 14.1, 19.6, 22.6, 22.6, 22.7, 22.7, 24.7, 24.7, 26.0, 26.0, 28.0, 29.3, 29.3, 29.4, 29.6, 29.6, 29.7, 29.8, 31.9, 36.5, 37.4, 37.5, 39.3, 39.4, 67.5, 69.3, 69.4, 71.7, 99.5, 104.3, 111.4, 113.8, 118.3, 149.4, 149.5, 153.4 ppm; IR (neat, NaCl): $\tilde{\nu}$ = 3191, 3157, 3111 (br, N–H), 1590, 1505 (C=N, Ar C–C), 1259 cm^{-1} (C–O); MS (MALDI): *m/z*: 1002.1 [M^+]; elemental analysis calcd for $C_{65}H_{112}N_2O_5$: C 77.95, H 11.27, N 2.80; found: C 78.08, H 11.35, N 2.61.

5(*S*): Eluent: CH_2Cl_2/ethyl acetate (20:1); yield: 20%; ^{1}H NMR (400 MHz, $CDCl_3$): δ = 0.87 (d, *J* = 6.8 Hz, 30H), 0.93–0.97 (m, 15H), 1.10–1.21 (m, 30H), 1.45–1.77 (m, 15H), 1.78–1.94 (m, 5H), 3.97–4.15 (m, 10H), 6.68 (s, 1H), 7.20 (dd, *J* = 8.2, 2.0 Hz, 1H), 7.24 ppm (d, *J* = 2.0 Hz, 1H); ^{13}C NMR (100 MHz, $CDCl_3$): δ = 19.6, 19.7, 19.7, 22.6, 22.6, 22.7, 24.7, 24.7, 28.0, 29.7, 29.8, 29.9, 36.2, 36.3, 36.5, 37.7, 37.5, 39.3, 39.3, 39.4, 67.5, 67.6, 67.7, 71.7, 99.6, 104.4, 111.3, 113.7, 118.3, 123.9, 126.7, 138.6, 149.4, 149.6, 153.5 ppm; IR (neat, NaCl): $\tilde{\nu}$ = 3140, 3108 (br, N–H), 1588, 1506 (C=N, Ar C–C), 1258 cm^{-1} (C–O); MS (MALDI): *m/z*: 1002.0 [M^+]; elemental analysis calcd for $C_{65}H_{112}N_2O_5$: C 77.95, H 11.27, N 2.80; found: C 78.15, H 11.38, N 2.76.

3(*S*)3C10: Eluent: hexane/ethyl acetate (10:1); yield: 39%; ^{1}H NMR (400 MHz, $CDCl_3$): δ = 0.86–0.92 (m, 27H), 0.92–0.94 (m, 9H), 1.07–1.41 (m, 54H), 1.41–1.61 (m, 9H), 1.61–1.94 (m, 15H), 3.94–4.14 (m, 12H), 6.68 (s, 1H), 6.90 ppm (s, 4H); ^{13}C NMR (100 MHz, $CDCl_3$): δ = 14.1, 19.6, 22.6, 22.7, 22.7, 24.7, 26.1, 28.0, 29.4, 29.4, 29.6, 29.8, 30.3, 31.9, 36.4, 37.4, 37.5, 39.3, 39.4, 67.5, 69.3, 71.7, 73.5, 100.0, 104.4, 104.5, 153.5 ppm; IR (neat, NaCl): $\tilde{\nu}$ = 3158, 3107 (br, N–H), 1590, 1500 (C=N, Ar C–C), 1236 cm^{-1} (C–O); MS (MALDI): *m/z*: 1158.1 [M^+]; elemental analysis calcd for $C_{75}H_{132}N_2O_6$: C 77.80, H 11.49, N 2.42; found: C 77.69, H 11.31, N 2.43.

6(*S*): Eluent: hexane/ethyl acetate (20:1); yield: 50%; ^{1}H NMR (400 MHz, $CDCl_3$): δ = 0.86 (d, *J* = 6.6 Hz, 36H), 0.92–0.95 (m, 18H), 1.08–1.40 (m, 36H), 1.46–1.65 (m, 12H), 1.65–1.80 (m, 6H), 1.81–1.92 (m, 6H), 3.96–4.11 (m, 12H), 6.69 (s, 1H), 6.91 ppm (s, 4H); ^{13}C NMR (100 MHz, $CDCl_3$): δ = 19.6, 22.6, 22.7, 24.7, 24.7, 28.0, 29.7, 29.9, 36.5, 37.4, 37.6, 39.3, 39.4, 67.6, 71.7, 100.0, 104.6, 126.3, 138.8, 153.6 ppm; IR (neat, NaCl): $\tilde{\nu}$ = 3146, 3107 (br, N–H), 1589, 1499 (C=N, Ar C–C), 1238 cm^{-1} (C–O); MS (MALDI): *m/z*: 1158.0 [M^+]; elemental analysis calcd for $C_{75}H_{132}N_2O_6$: C 77.68, H 11.49, N 2.42; found: C 77.69, H 11.25, N 2.47.

Acknowledgements

We thank the following institutions for financial support: Gobierno de Aragón (project PM068/2007), MICINN (Spain), FSE (UE) (projects MAT2006-13571-CO2-01, CTQ2006-15611-C02-01, and CTQ2008-03860) and MICINN CSIC-I3 (project 200860I054).

[1] D. N. Reindhout, *Supramolecular Materials and Technologies*, Wiley, New York, **1999**.
[2] F. J. M. Hoeben, P. Jonkheijm, E. W. Meijer, A. P. H. J. Schenning, *Chem. Rev.* **2005**, *105*, 1491–1546.
[3] K. Kinbara, T. Aida, *Chem. Rev.* **2005**, *105*, 1377–1400.
[4] J. A. A. W. Elemans, R. van Hameren, R. J. M. Nolte, A. E. Rowan, *Adv. Mater.* **2006**, *18*, 1251–1266.
[5] D. B. Amabilino, J. Veciana, *Top. Curr. Chem.* **2006**, *265*, 253–302.
[6] F. Vera, J. L. Serrano, T. Sierra, *Chem. Soc. Rev.* **2009**, *38*, 781–796.
[7] R. J. Bushby, O. R. Lozman, *Curr. Opin. Colloid Interface Sci.* **2002**, *7*, 343–354.
[8] T. Kato, N. Mizoshita, K. Kishimoto, *Angew. Chem.* **2006**, *118*, 44–74; *Angew. Chem. Int. Ed.* **2006**, *45*, 38–68.
[9] S. Kumar, *Chem. Soc. Rev.* **2006**, *35*, 83–109.
[10] S. Sergeyev, W. Pisula, Y. H. Geerts, *Chem. Soc. Rev.* **2007**, *36*, 1902–1929.
[11] S. Laschat, A. Baro, N. Steinke, F. Giesselmann, C. Hagele, G. Scalia, R. Judele, E. Kapatsina, S. Sauer, A. Schreivogel, M. Tosoni, *Angew. Chem.* **2007**, *119*, 4916–4973; *Angew. Chem. Int. Ed.* **2007**, *46*, 4832–4887.
[12] T. Kato, T. Yasuda, Y. Kamikawa, M. Yoshio, *Chem. Commun.* **2009**, 729–739.
[13] M. C. Foces-Foces, I. Alkorta, J. Elguero, *Acta Crystallogr. Sect. B* **2000**, *56*, 1018–1028.
[14] J. Barberá, R. Giménez, J. L. Serrano, *Adv. Mater.* **1994**, *6*, 470–472.
[15] J. Barberá, R. Giménez, J. L. Serrano, *Chem. Mater.* **2000**, *12*, 481–489.
[16] J. Barberá, A. Elduque, R. Giménez, L. A. Oro, J. L. Serrano, *Angew. Chem.* **1996**, *108*, 3048–3051; *Angew. Chem. Int. Ed. Engl.* **1996**, *35*, 2832–2835.
[17] J. Barberá, A. Elduque, R. Giménez, F. J. Lahoz, J. A. López, L. A. Oro, J. L. Serrano, *Inorg. Chem.* **1998**, *37*, 2960–2967.
[18] E. Cavero, S. Uriel, P. Romero, J. L. Serrano, R. Giménez, *J. Am. Chem. Soc.* **2007**, *129*, 11608–11618.
[19] R. Giménez, A. Elduque, J. A. López, J. Barberá, E. Cavero, I. Lantero, L. A. Oro, J. L. Serrano, *Inorg. Chem.* **2006**, *45*, 10363–10370.
[20] S. T. Heller, S. R. Natarajan, *Org. Lett.* **2006**, *8*, 2675–2678.
[21] J. Barberá, C. Cativiela, J. L. Serrano, M. M. Zurbano, *Liq. Cryst.* **1992**, *11*, 887–897.
[22] See, for example: a) D. M. Collard, C. P. Lillya, *J. Am. Chem. Soc.* **1991**, *113*, 8577–8583; b) S. T. Trzaska, H.-F. Hsu, T. M. Swager, *J. Am. Chem. Soc.* **1999**, *121*, 4518–4519; c) K. Kishikawa, S. Furusawa, T. Yanaki, S. Kohmoto, M. Yamamoto, K. Yamaguchi, *J. Am. Chem. Soc.* **2002**, *124*, 1597–1605.
[23] B. Glüsen, W. Heitz, A. Kettner, J. H. Wendorff, *Liq. Cryst.* **1996**, *20*, 627–633.
[24] A. Fechtenkötter, N. Tchebotareva, M. Watson, K. Mullen, *Tetrahedron* **2001**, *57*, 3769–3783.
[25] A. M. Levelut, *J. Phys. Lett.* **1979**, *40*, 81–84.
[26] A. M. Levelut, P. Oswald, A. Ghanem, J. Malthête, *J. Phys. Lett.* **1984**, *45*, 745–754.
[27] A. M. Levelut, J. Malthête, A. Collet, *J. Phys. Lett.* **1986**, *47*, 351–357.
[28] F. Livolant, A. M. Levelut, J. Doucet, J. P. Benoit, *Nature* **1989**, *339*, 724–726.

[29] J. Barberá, E. Cavero, M. Lehmann, J. L. Serrano, T. Sierra, J. T. Vázquez, *J. Am. Chem. Soc.* **2003**, *125*, 4527–4533.
[30] J. Barberá, M. Bardají, J. Jiménez, A. Laguna, M. P. Martínez, L. Oriol, J. L. Serrano, I. Zaragozano, *J. Am. Chem. Soc.* **2005**, *127*, 8994–9002.
[31] J. Barberá, J. Jiménez, A. Laguna, L. Oriol, S. Pérez, J. L. Serrano, *Chem. Mater.* **2006**, *18*, 5437–5445.
[32] I. Alkorta, J. Elguero, C. Foces-Foces, L. Infantes, *Arkivoc* **2006**, *ii*, 15–30.
[33] M. C. Torralba, M. Cano, J. A. Campo, J. V. Heras, E. Pinilla, M. R. Torres, *J. Organomet. Chem.* **2002**, *654*, 150–161.
[34] A. L. Llamas-Saiz, C. Foces-Foces, F. H. Cano, P. Jiménez, J. Laynez, W. Meutermans, J. Elguero, H.-H. Limbach, F. Aguilar-Parrilla, *Acta Crystallogr. Sect. B* **1994**, *50*, 746–762.
[35] F. Aguilar-Parrilla, C. Cativiela, M. D. Díaz de Villegas, J. Elguero, C. Foces-Foces, J. I. García, F. H. Cano, H.-H. Limbach, J. A. S. Smith, C. Toiron, *J. Chem. Soc. Perkin Trans. 2* **1992**, 1737–1742.
[36] R. G. Raptis, R. J. Staples, C. King, J. P. Fackler, *Acta Crystallogr. Sect. C* **1993**, *49*, 1716–1719.
[37] S. T. Trzaska, H. Zheng, T. M. Swager, *Chem. Mater.* **1999**, *11*, 130–134.

Received: April 30, 2009
Published online: July 27, 2009

